Journal of the Optical Society of America B

OPTICAL PHYSICS

Stability properties of an Rb CPT atomic clock with buffer-gas-free cells under dynamic excitation

SERGEY KOBTSEV, DABA RADNATAROV,* SERGEY KHRIPUNOV, IVAN POPKOV, VALERII ANDRYUSHKOV, AND TATIANA STESHCHENKO

Novosibirsk State University, Pirogova str., 2, Novosibirsk, 630090, Russia
**Corresponding author: d.radnatarov@gmail.com*

Received 11 June 2019; revised 14 August 2019; accepted 15 August 2019; posted 15 August 2019 (Doc. ID 369834); published 10 September 2019

This work presents a study of the short-term stability properties of Rb atomic clocks based on coherent population trapping (CPT) under dynamic excitation of a CPT resonance in cells without buffer gas. It is demonstrated that in an optical cell with anti-relaxation coating of its inner walls, the best stability is achieved at the scanning frequency of the frequency difference of the bichromatic pump field equal to 2 kHz at the resonance width of 450 Hz. In cells without a wall coating, the optimal scanning frequency range is found to be 1.2–2.8 kHz at the resonance width of 29 kHz. Examination of the slope of the stabilization system's discriminant curve at zero error signal for buffer-gas-free cells uncovered an amount of correlation between the discriminant curve slope and atomic clock stability. It is demonstrated that the highest stability of atomic clocks in dynamic excitation mode is achieved at a ratio of scanning frequency and amplitude around 1.

https://doi.org/10.1364/JOSAB.36.002700

1. INTRODUCTION

Frequency standards relying on coherent population trapping (CPT) resonance are widely used in diverse applications [1,2]. Strong demand for such frequency standards along with their undeniable merits (compact dimensions as well as low weight and power consumption) encourage continued efforts to improve their performance and, in particular, to seek ways of improving their main parameter: output frequency stability. One of the ways to improve the relative frequency stability of atomic clocks based on CPT resonance is formation of the resonance so as to simultaneously optimize both the resonance width and its signal-to-noise (S/N) ratio [3].

A CPT resonance is formed when the frequency difference of a bichromatic pumping field is scanned around the value equal to the frequency of hyperfine transition of the ground state of an alkali metal atom. Both scanning frequency and amplitude define the mode of resonance formation. Two general distinct types of CPT resonance formation can be distinguished: quasi-stationary mode when the scanning frequency is low ($< 1 - 10$ Hz) and dynamic mode in which the scanning frequency is relatively high (> 100 Hz). This differentiation between modes by scanning frequency is qualitative rather than quantitative and essentially means that in the quasi-stationary mode, the cell transmittance only depends on the frequency difference between the components of the bichromatic pumping field, and thus the CPT resonance parameters do not depend on the scanning frequency. Conversely, in the dynamic mode, the cell transmittance depends not only on the frequency difference of the pumping field components but also on the scanning frequency [4,5].

Dynamic CPT resonance formation, which is essentially a method of frequency modulation spectroscopy [6], allows a better S/N ratio due to recording of the resonance within a higher scan frequency range where spectral noise density is normally reduced [7]. However, improvement of this parameter as the frequency is raised is inevitably accompanied by simultaneous degradation of the CPT resonance quality: its width grows, its amplitude is reduced, and its shape is deformed [4,8]. The difference between the rates at which the S/N ratio and CPT resonance quality evolve may lead to improvement in frequency stability of atomic clocks and thus fuel interest in dynamic formation of CPT resonances. It was earlier demonstrated that atomic clock stability depends on the parameters of resonance scanning and that such dependence exists in clocks using cells both with [9,10] and without [11–13] a buffer gas, as well as in atomic clocks using caesium beams [14]. However, the question of how distortion of the CPT resonance shape at higher frequencies affects the short-term stability properties of atomic clocks has never been experimentally studied in detail.

The objective of the present work consists of exploration of the dynamic mode of CPT resonance formation under new conditions: in optical cells devoid of buffer gas. We studied rubidium vapor cells with and without anti-relaxation coating of their inner walls. These two types of cells exhibited diametrically opposite behavior in relation to the time of coherent interaction of polarized atoms with the field: in cells with anti-relaxation coating, the depolarization probability of an atom upon collision with the walls is generally reduced by 3–6 orders of magnitude [15,16] compared to cells without such coating, in which collisions of an active atom with the wall result in total randomization of its spin orientation. Since the coherence preservation time of the atomic ground state determines the CPT resonance quality, buffer-gas-free cells with and without anti-relaxation coating of their inner walls enabled study of atomic clock stability at extreme values of the CPT resonance width (close to the broadest and the narrowest) corresponding to substantially different qualities of the quantum discriminator. Study of stability properties of Rb CPT atomic clocks in these two extreme cases is beneficial for establishment of general patterns under dynamic excitation.

It is pertinent to note that buffer-gas-free cells with anti-relaxation coatings so far have not been used in commercial atomic clocks due to a number of problems, of which the gravest is decomposition of the anti-relaxation coating at high temperatures required by anodic bonding process [17] used in micro-fabrication of vapor cells [18]. Presently, anti-relaxation-coated cells are still based on the conventional glass-blowing technology, even though this may change in the near future. Recent progress in low-temperature technologies of gas cell fabrication [19,20] and anti-relaxation coatings with relatively high melting point [21,22] substantially facilitated technological development of fabrication of alkali vapor cells equipped with an anti-relaxation wall coating [23]. Advancement of these technologies takes on a particular significance in fabrication of millimeter (mm)-scale cells, which requires relatively high pressure of the buffer gas, ensuring a narrow CPT resonance, but at the same time greatly reducing its contrast [21]. This contrast reduction necessitates detection methods, which are able to provide relatively high S/N ratio at low CPT resonance contrast. Formation of a CPT resonance in dynamic excitation mode is one of such methods, although it is not sufficiently studied in the case of buffer-gas-free cells with anti-relaxation coatings.

This work reports on detailed experimental study of atomic clock stability under dynamic excitation of a broad variety of CPT resonances with differing quality in buffer-gas-free cells. Our main objective was to find out how significantly atomic clock stability can be affected solely by changing parameters of dynamics of CPT resonance excitation.

2. EXPERIMENT

Our experimental work on dynamic excitation of CPT resonances was carried out on the installation schematically shown in Fig. 1. The CPT resonance in ^{87}RP vapor was excited with a semiconductor laser whose output spectrum contained two frequencies 6.835 GHz apart, which corresponds to the transition frequency between the sub-levels of hyperfine ^{87}RP ground level splitting. Frequency difference (FD) equal to 6.835 GHz

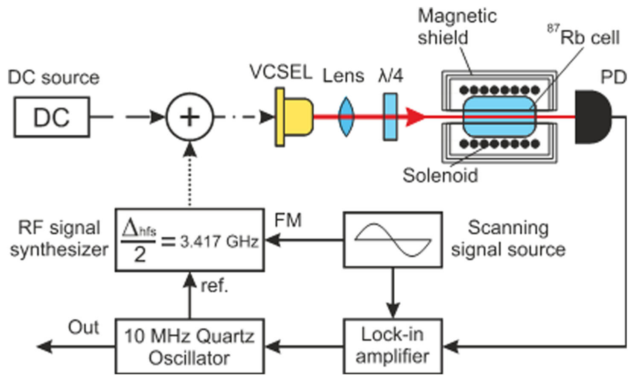

Fig. 1. Layout of the experimental installation for studies of dynamic formation of CPT resonances.

was generated through the sideband technique by modulation of the injection current of a single-frequency semiconductor laser at the frequency of 3.417 GHz. The input power of the RF signal (3.417 GHz) was chosen from the condition of creating such side-band amplitude, at which the CPT resonance light shift was minimized [24–27].

Linearly polarized 50 µW output of a vertical-cavity surface-emitting laser (VCSEL) from Oclaro with 100 MHz linewidth at 795 nm was collimated with an aspherical lens into a 2 mm beam whose polarization was converted into circular by a quarter-wave phase plate. The intensity of radiation propagated through a cell filled with ^{87}RP vapor was registered with a photodetector (PD). The 10 mm cell had anti-reflection coating on the inner walls and was placed inside a solenoid that created a 100 mG magnetic field parallel to the beam for Zeeman splitting of the ground state of Rb and further enclosed in a three-layer μ-metal magnetic shield to isolate the cell from external magnetic fields. Paraffin was used as the material for anti-relaxation coating [21,28]; however, other anti-relaxation materials are also applicable [25,29,30]. The cell temperature was stabilized at approximately 333 K to the precision of 1 mK. The bichromatic field FD was scanned around the value of 6.835 GHz with the aid of a sine wave generator. Figure 2 provides an example of a typical CPT resonance created in a cell with an anti-relaxation coating in quasi-stationary mode (scanning frequency of 1 Hz). The width (FWHM) of the narrow resonance peak at low scan frequency was measured at 460 Hz (with 1.6% contrast). As the scanning frequency was increased (Fig. 3), the narrow resonant peak broadened, and oscillations emerged on the rear slope of the resonant curve, which grew with the scanning frequency

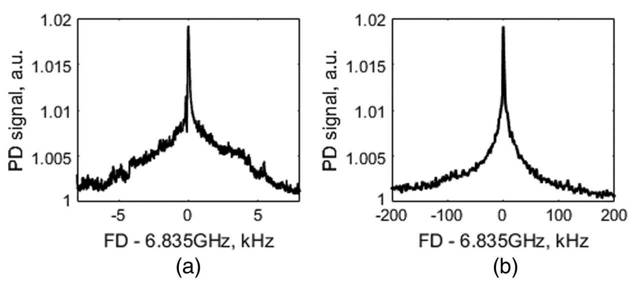

Fig. 2. Typical shape of a CPT resonance formed under quasi-stationary excitation in a cell (a) with anti-relaxation coating and (b) without coating.

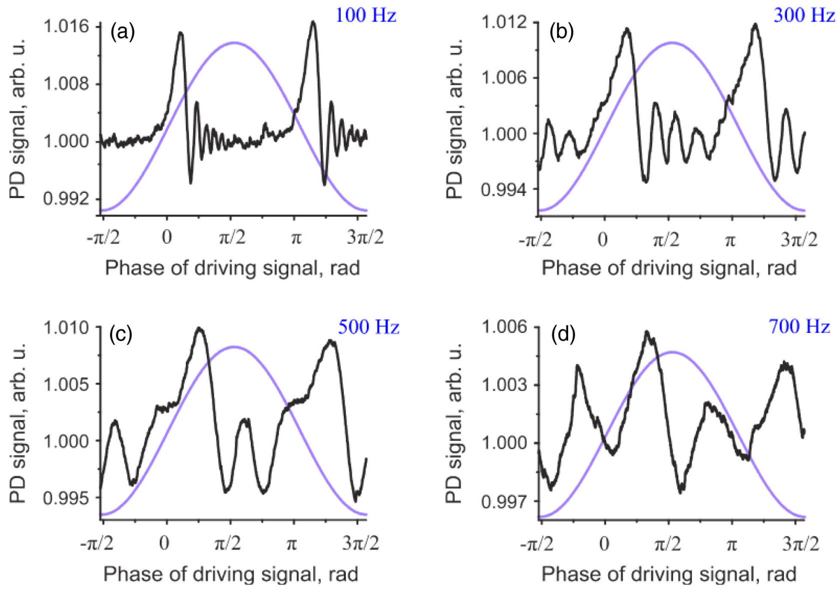

Fig. 3. Evolution of the narrow CPT resonance peak as a function of the scanning frequency equal to: (a) 100 Hz, (b) 300 Hz, (c) 500 Hz, (d) 700 Hz. The violet curve corresponds to the sine wave driving the CPT resonance scanning; the horizontal axis is given in phase units of this control signal.

and affected the resonance shape [4]. The CPT resonance in a cell of similar dimensions but without any coating of the inner walls was notably wider: at the scanning frequency of 1 Hz, its width amounted to 29 kHz (with 1.8% contrast) Fig. 2(b). The scanning amplitude corresponded to the ranges given in Fig. 2. For the coated cell it was 15 kHz (peak-to-peak) and 400 kHz (peak-to-peak) for the uncoated cell. This amplitude was chosen from the condition that at the edges of the scanning range, the photodetector signal ceased to depend on the frequency of the RF source. A higher level of noise in the case of the coated cell comes from higher visibility of frequency fluctuations of the quartz oscillator within a narrower CPT resonance.

In order to obtain short-term stability of the atomic clock, we measured the Allan deviation over 1 s with the modulation frequency and amplitude covering the range of 0.5–3.0 kHz and 0.6–4.0 kHz, respectively. A total of over 60 measurements were carried out for each of the cells in order to generate a map of Allan deviation distribution. The measurement results are presented in Fig. 4. In the cell with anti-relaxation coating [Fig. 4(a)], the highest short-term stability of 3×10^{-11} was achieved at both the modulation frequency and modulation amplitude equal to 2 kHz. The stability measurement error was governed by the instability of the rubidium frequency reference included into the frequency comparator (Ruknar Ch7-1011) and equalled 1×10^{-11} over 1 s, whereas the accuracy of measurement of the comparator frequency instability was 1×10^{-12} over 1 s. It can be seen from Fig. 4 that there is an optimum relation between the frequency and amplitude at the frequency/amplitude ratio around 1.0. This is because the CPT resonance width grows in parallel with the scanning frequency, and a broader resonance requires larger scanning amplitude to maximize the error signal. Analogous optimal value of the frequency/amplitude ratio is observed for cells without wall coating [Fig. 4(b)]. However, in an uncoated cell,

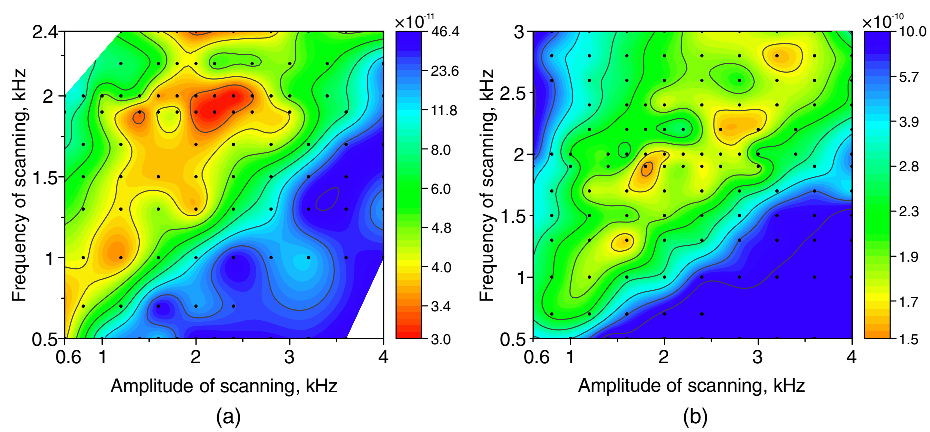

Fig. 4. Atomic clock stability under dynamic CPT resonance formation in Rb vapor: (a) anti-relaxation-coated cell and (b) uncoated cell. Black dots mark measured data points with the rest of the map recreated via an interpolation routine.

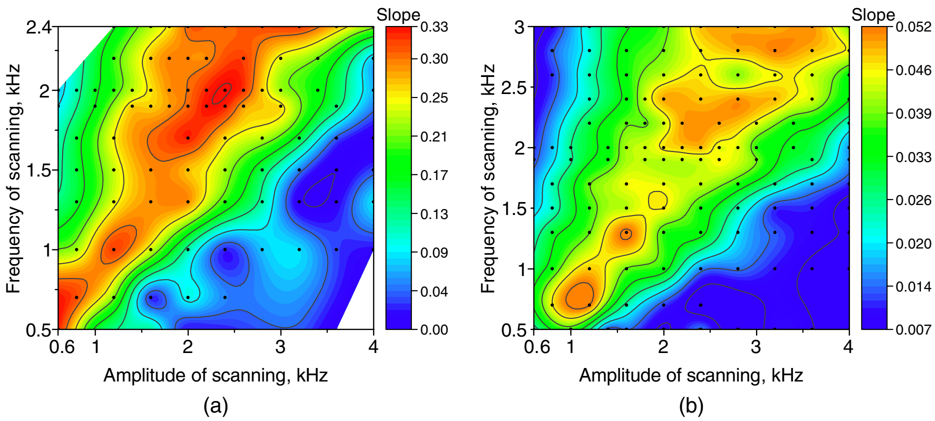

Fig. 5. Discriminant curve slope at zero error signal in dynamic CPT resonance formation mode: (a) anti-relaxation-coated cell and (b) uncoated cell. Black dots mark measured data points with the rest of the map recreated via an interpolation routine.

there is no defined stability maximum. In this case, best results could be achieved at different scan frequencies within the range of 1.2–2.8 kHz, and they did not exceed 1.5×10^{-10} for this particular cell.

It was also interesting to find out experimentally how the slope of the discriminant curve formed from the CPT signal and used in the atomic clock stabilization feedback system evolves as a function of scanning frequency. To determine the discriminant curve slope, the feedback loop was broken and the error signal change produced by deviation of FD by 1 Hz from the central value of 6.835 GHz was measured. The quartz generator used to create a signal at 3.417 GHz whose frequency was stabilized in the above-mentioned experiments had instability at the level of 1×10^{-10} over 1 s. Therefore, in the experiment on measurement of the discriminant curve slope, we used an atomic frequency standard with stability 1×10^{-11} over 1 s to form the signal at 3.417 GHz. The slope measurements were done for the same set of modulation parameters as the stability measurements. The results of experimental measurement of the discriminant curve slope around zero error signal for both cells are given in Fig. 5.

Figure 5 manifests certain correlation of the discriminant curve slope and the atomic clock stability within a relatively high-frequency scanning range around 2 kHz.

However, analysis of the low-frequency range (0.5–1.5 kHz) shows that relatively steep slope of the discriminant curve does not translate into high atomic clock stability. The main factor behind this behavior is the S/N ratio, which is higher at higher scanning frequencies. This improves atomic clock stability at relatively high scan frequencies due to being inversely proportional to the S/N ratio [31].

From Fig. 5, it can be seen that for both studied cells (with and without an anti-relaxation coating), the steepest discriminant curve slope is reached at the ratio of the modulation frequency to the modulation amplitude close to unity. This suggests that the established optimal ratio is generally valid for buffer-gas-free cells.

Given in Fig. 6 are the averaging-time dependencies of the Allan deviation for both types of the used cells (with and without coating). It is evident that over the 1–1000 s temporal averaging scale, the Allan deviation duly drops off as a square root of average time.

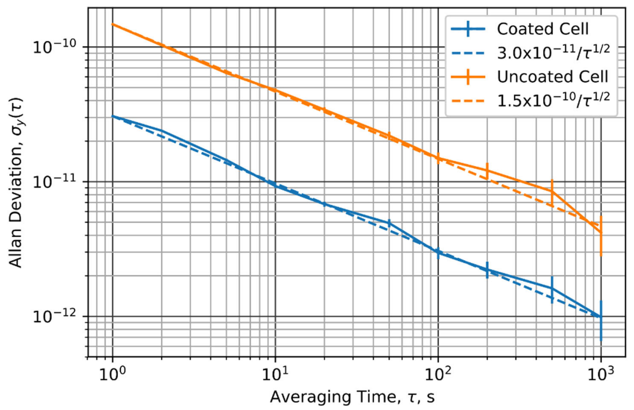

Fig. 6. Plots of the Allan deviation within the 1–1000 s temporal averaging scale for the most stable regions of Figs. 4(a) and 4(b), marked with red [Fig. 4(a)] and orange [Fig. 4(b)] colors.

3. CONCLUSION

This work presents the results of research in stability of atomic clocks relying on CPT resonances dynamically formed within a broad range of scanning frequencies and amplitudes in buffer-gas-free cells. In a cell with anti-relaxation coating of its inner walls, the best stability of 3×10^{-11} over 1 s was observed at the scanning frequency of 2 kHz, whereas in an uncoated cell, the highest stability of 1.5×10^{-10} over 1 s was reached at several frequencies within the scan frequency range of 1.2–2.8 kHz. The optimal scan frequency range corresponds to the minimal Allan deviation, which is inversely proportional to the product $Q\times$ (S/N ratio) [1], where Q is the CPT resonance linear quality factor depending upon the CPT resonance width $\Delta\nu$ as $Q \propto 1/\Delta\nu$ [14]. As the scan frequency is raised, the CPT resonance quality drops (the resonance width grows and oscillations emerge on the rear resonance slope as shown in Fig. 3), but its S/N ratio improves and thus leads to an optimal range of scan frequencies, where the highest value of the product $Q\times$ (S/N ratio) is achieved.

It is important to emphasize that the stability figures measured in the present work are not the best achieved for similar devices [32]. Moreover, setting stability records was not among our objectives (atomic clock short-term stability of

$X \times \tau\ 10^{-11}\tau^{-1/2}$ may be considered both as average and close to the best possible, depending on the optical cell dimensions [33,34]). Our primary goal was to learn how strongly the parameters of dynamics of CPT resonance excitation affect the stability of atomic clocks. The answer resulting from the present work may be summarized as follows: dynamics of CPT resonance excitation may improve atomic clock stability but, in our view, not significantly (at the level of tens of percentage points). Furthermore, this improvement requires that the scan frequency be approximately equal to the scan amplitude.

Funding. Russian Science Foundation (16-12-10147); Ministry of Education and Science of the Russian Federation (3.889.2017/PHC).

Acknowledgment. V. Andryushkov was supported by the Grant of the Ministry of Education and Science of the Russian Federation.

REFERENCES

1. J. Vanier, C. Tomescu, and C. Tomescu, *The Quantum Physics of Atomic Frequency Standards* (CRC Press, 2015).
2. J. Kitching, "Chip-scale atomic devices," Appl. Phys. Rev. **5**, 031302 (2018).
3. V. Shah and J. Kitching, "Advances in coherent population trapping for atomic clocks," in *Advances in Atomic, Molecular and Optical Physics*, E. Arimondo, P. R. Berman, and C. C. Lin, eds. (Elsevier, 2010), Vol. **59**, pp. 21–74.
4. S. A. Khripunov, D. A. Radnatarov, S. M. Kobtsev, V. I. Yudin, A. V. Taichenachev, M. Y. Basalaev, M. V. Balabas, V. A. Andryushkov, and I. D. Popkov, "Transient processes under dynamic excitation of a coherent population trapping resonance," Quantum Electron. **46**, 668 (2016).
5. V. I. Yudin, A. V. Tichenachev, M. Y. Basalaev, and D. V. Kovalenko, "Dynamic regime of coherent population trapping and optimization of frequency modulation parameters in atomic clocks," Opt. Express **25**, 2742–2751 (2017).
6. J. M. Supplee, E. A. Whittaker, and W. Lenth, "Theoretical description of frequency modulation and wavelength modulation spectroscopy," Appl. Opt. **33**, 6294–6302 (2009).
7. V. Gerginov, S. Knappe, S. Shah, L. Hollberg, and J. Kitching, "Laser noise cancellation in single-cell CPT clocks," IEEE Trans. Instrum. Meas. **57**, 1357–1361 (2008).
8. D. Radnatarov, S. Khripunov, S. Kobtsev, A. Taichenachev, V. Yudin, M. Basalaev, I. Popkov, and V. Andryushkov, "Effect of electromagnetically-induced transparency delay generated by dynamic coherent population trapping in Rb vapour," Proc. SPIE **9763**, 97630A (2016).
9. I. Ben-Aroya, M. Kahanov, and G. Eisenstein, "Optimization of FM spectroscopy parameters for a frequency locking loop in small scale CPT based atomic clocks," Opt. Express **15**, 15060–15065 (2007).
10. M. Kahanov, I. Ben-Aroya, and G. Eisenstein, "Dependence of small-scale atomic clock performance on frequency modulation parameters used in the frequency control loop," Opt. Lett. **33**, 944–946 (2008).
11. S. Khripunov, D. Radnatarov, and S. Kobtsev, "Atomic clock based on a coherent population trapping resonance in ^{87}Rb with improved high-frequency modulation parameters," Proc. SPIE **9378**, 93780A (2015).
12. S. M. Kobtsev, D. Radnatarov, S. Khripunov, I. Popkov, V. Andryushkov, and T. Steschenko, "Atomic clock stability under dynamic excitation of coherent population trapping resonance in cells without buffer gas," Proc. SPIE **10548**, 1054820 (2018).
13. J. P. Mcgilligan, "Micro-fabricated diffractive optics for quantum sensors and atomic clocks," Ph.D. thesis (University of Strathclyde, 2017).
14. J. Vanier and C. Audoin, "5.4. Determination of the frequency of the atomic resonance," in *The Quantum Physics of Atomic Frequency Standards* (1989), Vol. **2**, pp. 708–752.
15. T. Bandi, C. Affolderbach, and G. Mileti, "Laser-pumped paraffin-coated cell rubidium frequency standard," J. Appl. Phys. **111**, 124906 (2012).
16. M. T. Graf, D. F. Kimball, S. M. Rochester, K. Kerner, C. Wong, D. Budker, E. B. Alexandrov, M. V. Balabas, and V. V. Yashchuk, "Relaxation of atomic polarization in paraffin-coated cesium vapor cells," Phys. Rev. A **72**, 25–28 (2005).
17. J. A. Dziuban, *Bonding in Microsystem Technology* (Springer, 2006).
18. P. Knapkiewicz, "Technological assessment of MEMS alkali vapor cells for atomic references," Micromachines **10**, 25 (2019).
19. R. Straessle, M. Pellaton, C. Affolderbach, Y. Pétremand, D. Briand, G. Mileti, and N. F. De Rooij, "Low-temperature indium-bonded alkali vapor cell for chip-scale atomic clocks," J. Appl. Phys. **113**, 064501 (2013).
20. S. Kobtsev, S. Donchenko, S. Khripunov, D. Radnatarov, I. Blinov, and V. Palchikov, "CPT atomic clock with cold-technology-based vapour cell," Opt. Laser Technol. **119**, 105634 (2019).
21. S. J. Seltzer and M. V. Romalis, "High-temperature alkali vapor cells with antirelaxation surface coatings," J. Appl. Phys. **106**, 114905 (2009).
22. M. Bhattarai, V. Bharti, V. Natarajan, A. Sargsyan, and D. Sarkisyan, "Study of EIT resonances in an anti-relaxation coated Rb vapor cell," Phys. Lett. A **383**, 91–96 (2019).
23. R. Straessle, M. Pellaton, C. Affolderbach, Y. Pétremand, D. Briand, G. Mileti, and N. F. De Rooij, "Microfabricated alkali vapor cell with anti-relaxation wall coating," Appl. Phys. Lett. **105**, 043502 (2014).
24. M. Zhu and L. S. Cutler, "Theoretical and experimental study of light shift in a CPT-based Rb vapor cell frequency standard," in *32nd Annual Precise Time and Time Interval Meeting* (2000), pp. 311–323.
25. F. Levi, A. Godone, and J. Vanier, "The light shift effect in the coherent population trapping cesium maser," in *IEEE Transactions on Ultrasonics, Ferroelectrics and Frequency Control* (2000), Vol. **47**, pp. 466–470.
26. J. Vanier, A. Godone, and F. Levi, "Coherent microwave emission in coherent population trapping: origin of the energy and of the quadratic light shift," in *Joint Meeting of the European Frequency and Time Forum and the IEEE International Frequency Control Symposium (Cat. No. 99CH36313)* (IEEE, 1999), Vol. **1**, pp. 96–99.
27. S. Kobtsev, D. Radnatarov, S. Khripunov, I. Popkov, V. Andryushkov, T. Steshchenko, V. Lunin, and Y. Zarudnev, "Feedback-controlled and digitally processed coherent population trapping resonance conversion in ^{87}Rb vapour to high-contrast resonant peak," New J. Phys. **19**, 043016 (2017).
28. M. A. Bouchiat and J. Brossel, "Relaxation of optically pumped Rb atoms on paraffin-coated walls," Phys. Rev. **147**, 41–54 (1966).
29. M. V. Balabas, K. Jensen, W. Wasilewski, H. Krauter, L. S. Madsen, J. H. Müller, T. Fernholz, and E. S. Polzik, "High quality anti-relaxation coating material for alkali atom vapor cells," Opt. Express **18**, 5825–5830 (2010).
30. M. V. Balabas, T. Karaulanov, M. P. Ledbetter, and D. Budker, "Polarized alkali-metal vapor with minute-long transverse spin-relaxation time," Phys. Rev. Lett. **105**, 4–7 (2010).
31. R. Lutwak, D. Emmons, T. English, W. Riley, C. Stark, D. K. Serkland, and G. M. Peake, "The chip-scale atomic clock–recent development progress," in *34th Annual Precise Time and Time Interval Systems and Applications Meeting* (2003), pp. 1–12.
32. M. A. Hafiz, G. Coget, M. Petersen, C. Rocher, S. Guérandel, T. Zanon-Willette, E. Clercq, and R. Boudot, "Toward a high-stability coherent population trapping Cs vapor-cell atomic clock using autobalanced Ramsey spectroscopy," Phys. Rev. Appl. **9**, 064002 (2018).
33. Y. Zhao, S. Tanner, A. Casagrande, C. Affolderbach, L. Schneller, G. Mileti, and P. A. Farine, "CPT cesium-cell atomic clock operation with a 12-mW frequency synthesizer ASIC," IEEE Trans. Instrum. Meas. **64**, 263–270 (2015).
34. P. Yun, F. Tricot, C. E. Calosso, S. Micalizio, B. François, R. Boudot, S. Guérandel, and E. De Clercq, "High-performance coherent population trapping clock with polarization modulation," Phys. Rev. Appl. **7**, 014018 (2017).